


One-loop electroweak radiative corrections to lepton pair production in polarized electron-positron collisions

S. Bondarenko^{✉*}*Bogoliubov Laboratory of Theoretical Physics, JINR, Dubna 141980 Russia*Ya. Dydyshka^{✉,†}, L. Kalinovskaya[✉], R. Sadykov[✉], and V. Yermolchyk^{✉,†}*Dzhelepov Laboratory of Nuclear Problems, JINR, Dubna 141980 Russia* (Received 12 May 2020; accepted 31 July 2020; published 24 August 2020)

This paper presents high-precision theoretical predictions for s-channel $e^+e^- \rightarrow l^-l^+$ scattering. The calculations are performed using the SANC system. They take into account complete one-loop electroweak radiative corrections as well as the longitudinal polarization of the initial beams. The reaction observables are obtained using the helicity amplitude method with taking into account the initial- and final-state fermion masses. Numerical results are given for the center-of-mass energy range $\sqrt{s} = 250\text{--}1000$ GeV with various degrees of polarization.

DOI: [10.1103/PhysRevD.102.033004](https://doi.org/10.1103/PhysRevD.102.033004)

I. INTRODUCTION

Planned experiments (with/without polarization of the initial beams) in high energy physics for electron-positron annihilation have been proposed with the capability of precise measurements at the International Linear Collider (ILC) [1–7], the e^+e^- Future Circular Collider (FCC-ee) [8–12], the Compact Linear Collider (CLIC) [13–15], and the Circular Electron Positron Collider (CEPC) [16].

The high precision of experiments at future e^+e^- colliders demands nontrivial requirements for theory, which are reviewed in [17]. The first calculation of corrections to the $e^+e^- \rightarrow \mu^-\mu^+$ process was carried out by Passarino and Veltman [18]. Most of the theoretical works on lepton pair production (LPP) before the large electron-positron (LEP) collider era concerned the next-to-leading order electroweak (EW) radiative corrections (RCs) (see, e.g., [19–24]).

The above-mentioned calculations were an evolution of basic codes incorporated in the standard LEP tools such as TOPAZO [25–27], ZFITTER [28], and ALIBABA [29,30]. A comprehensive review of the underlying theory and methods which have been used to create these codes can be found in the monograph [31].

*bondarenko@jinr.ru

†Also at Institute for Nuclear Problems, Belarusian State University, Minsk, 220006 Belarus.

Published by the American Physical Society under the terms of the Creative Commons Attribution 4.0 International license. Further distribution of this work must maintain attribution to the author(s) and the published article's title, journal citation, and DOI. Funded by SCOAP³.

Polarized electron/positron beams are important to achieve relative uncertainty of measurements of the total cross section and left-right asymmetry with an accuracy of a few permille. In the LEP era, results were presented for theoretical support of the polarized e^+e^- annihilation; see [24,32–37]. However, the mentioned investigations did not create a tool at the same level accuracy for polarized beams.

The only exception are calculations of the KKMC event generator project [38–40], which provide differential and total cross sections for arbitrary polarizations of the initial e^+e^- beams and final-state fermions. The precision for unpolarized case is at the two to four permille level. The KKMC program includes the first order electroweak corrections in the spin amplitudes using technique of form factors in front of the invariant amplitudes in the matrix element [39]. The spin amplitudes are defined and used not only for a single hard photon but for an arbitrary number of hard photons using technique of Kleiss-Stirling [41], which employs Weyl spinor technique with arbitrary fermion spin quantization axis [38,39].

There are three main e^+e^- processes to be used for the purpose of high-precision luminometry at flavor factories and future colliders: Bhabha, LPP $e^+e^- \rightarrow l^-l^+$, and photon pair production $e^+e^- \rightarrow \gamma\gamma$ [42].

In a series of papers [43,44] and this paper, we recall the above-mentioned three processes taking into account the one-loop EW RC and longitudinally polarized e^+e^- initial beams.

At the moment, the most advanced and widely used generators with one-loop RCs for estimation of luminosity by LPP process are BABAYAGA [45–48] and KKMC [39,49].

For the unpolarized case, we have already presented a comprehensive comparison of the $e^+e^- \rightarrow f\bar{f}$ process with

the results of ZFITTER for all light fermion production channels in [50]. In this work, we give a brief description, focusing on the high energy region, of the calculation of EW RCs for the lepton (muon) pair production including the contributions of the longitudinal polarization of the initial states.

In the future e^+e^- collider program, the optimized accelerator parameters are the center-of-mass (c.m.) energy of 250 GeV, and higher and longitudinal electron $\pm 80\%$ and positron $0, \pm 30\%$ degree of polarization. Moreover, it proposes a balance between polarization and c.m. energy sets for optimal physics diversity.

In this study, the relevant contributions to the cross section are calculated analytically using the helicity amplitudes approach, which allows one to evaluate the contribution of any polarization of the initial and final fermions, and then obtain a numerical result. The helicity amplitudes were used not only for the Born-like parts but also for the hard photon bremsstrahlung contribution taking into account the initial and final masses of the radiated particles. In this paper, we, to be specific, consider only longitudinally polarized initial beams for experimental conditions of future colliders [7, 15, 51]. The angular and energy dependence is also considered.

In a special case of the LPP $e^+e^- \rightarrow \tau^-\tau^+$ reaction, the τ lepton decays can be used to determine their polarization [52], which gives extra information on the $Z\tau\tau$ vertex. The influence of the polarization of the initial beams to the asymmetries and the final lepton polarization is given in [53].

There are many papers devoted to the study of the $e^+e^- \rightarrow \mu^+\mu^-$ channel at the one-loop level with polarized effects in the initial state; see, e.g., [33, 34] and references therein. It is highly nontrivial to perform a tuned comparison of the numerical results, since the authors not always present a complete list of input parameters.

We have performed high-precision tests at the tree level using the electron-positron branch of the MCSANC integrator [54, 55] and the generator RENESANCE [56] with the results of alternative codes. The polarized Born and hard photon bremsstrahlung contributions were compared with the corresponding values obtained with the help of the CalcHEP [57] and WHIZARD packages [58–61]. The sum of virtual and soft photon bremsstrahlung contributions in the unpolarized case is compared with the AITALC-1.4 code [62].

Numerical estimations are presented for the total and differential cross sections in the scattering angle $\cos \vartheta_l$ and for relative corrections. Also, the left-right asymmetry A_{LR} is given.

Considering the $e^+e^- \rightarrow l^-l^+$ process as one for the purpose of luminometry, one needs to take into account high-order effects, such as leading multiphoton QED logarithms, EW, and mixed QCD-EW multiloop corrections. These corrections will be implemented in the future.

The paper is organized as follows. Section II is devoted to the expressions for the covariant amplitude (CA) and helicity amplitude (HA) for the Born, virtual, and hard photon bremsstrahlung contributions. The approach for estimating polarization effects is also given. Section III contains numerical results for the total and differential cross sections as well as for relative corrections and A_{LR} asymmetry. The comparison with other computer codes is also given. Finally, in Sec. IV, we present conclusions and outlook for further work on LPP process within the SANC framework.

II. DIFFERENTIAL CROSS SECTION

The cross section of the generic process $e^+e^- \rightarrow \dots$ of the longitudinally polarized e^+ and e^- beams with the polarization degrees P_{e^+} and P_{e^-} can be expressed as follows:

$$\sigma(P_{e^+}, P_{e^-}) = \frac{1}{4} \sum_{\chi_1, \chi_2} (1 + \chi_1 P_{e^+})(1 + \chi_2 P_{e^-}) \sigma_{\chi_1 \chi_2}, \quad (1)$$

where $\chi_{1(2)} = -1(+1)$ corresponds to the particle i with the left (right) helicity.

The complete one-loop cross section of the process can be split into four parts,

$$\sigma^{\text{one-loop}} = \sigma^{\text{Born}} + \sigma^{\text{virt}}(\lambda) + \sigma^{\text{soft}}(\lambda, \omega) + \sigma^{\text{hard}}(\omega), \quad (2)$$

where σ^{Born} is the Born cross section, σ^{virt} is the contribution of virtual (loop) corrections, $\sigma^{\text{soft(hard)}}$ is the soft (hard) photon emission contribution (the hard photon energy $E_\gamma > \omega$). Auxiliary parameters λ (“photon mass”) and ω are canceled after summation.

We apply the helicity approach to all the contributions.

The virtual (Born) cross section of the $e^+e^- \rightarrow l^-l^+$ process

$$e^+(p_1, \chi_1) + e^-(p_2, \chi_2) \rightarrow l^-(p_3, \chi_3) + l^+(p_4, \chi_4) \quad (3)$$

can be written as follows:

$$\frac{d\sigma_{\chi_1 \chi_2}^{\text{virt(Born)}}}{d \cos \vartheta_l} = \pi \alpha^2 \frac{\beta_l}{2s} |\mathcal{H}_{\chi_1 \chi_2}^{\text{virt(Born)}}|^2, \quad (4)$$

where

$$|\mathcal{H}_{\chi_1 \chi_2}^{\text{virt(Born)}}|^2 = \sum_{\chi_3 \chi_4} |\mathcal{H}_{\chi_1 \chi_2 \chi_3 \chi_4}^{\text{virt(Born)}}|^2. \quad (5)$$

m_l is the final lepton mass and $\beta_l = \sqrt{1 - \frac{4m_l^2}{s}}$, ϑ_l is the angle between the final lepton l^- and initial electron e^- .

The soft photon bremsstrahlung terms [initial-state radiation (ISR), interference (IFI), final-state radiation (FSR)] are factorized to the Born cross section as follows:

$$\begin{aligned}
\sigma^{\text{soft,ISR}} &= -\sigma^{\text{Born}} \frac{\alpha}{\pi} Q_e^2 \left\{ (1 + L_e) \ln \left(\frac{4\omega^2}{\lambda} \right) \right. \\
&\quad \left. + L_e \left(1 + \frac{1}{2} L_e \right) + \frac{\pi^2}{3} \right\}, \\
\sigma^{\text{soft,IFI}} &= \sigma^{\text{Born}} \frac{\alpha}{\pi} Q_e Q_l \left\{ 2 \ln d_l \ln \left(\frac{4\omega^2}{\lambda} \right) \right. \\
&\quad + \left[2 \ln \left(1 + \frac{d_l^2}{st} \right) + \ln \left(-\frac{st}{d_l^2} \right) \right] \ln \left(-\frac{st}{d_l^2} \right) \\
&\quad + \left[2J_l - \ln \left(1 - \frac{2m_l^2}{\beta_l^+ d_l} \right) \right] \ln \left(1 - \frac{2m_l^2}{\beta_l^+ d_l} \right) \\
&\quad + 2\text{Li}_2 \left(1 + \frac{2t}{\beta_l^+ d_l} \right) - 2\text{Li}_2 \left(-\frac{d_l^2}{st} \right) \\
&\quad \left. - 2\text{Li}_2 \left(\frac{\beta_l^- d_l}{(m_l^2 + t) - \beta_l^- d_l} \right) \right\} - \left\{ t \leftrightarrow u \right\}, \\
\sigma^{\text{soft,FSR}} &= -\sigma^{\text{Born}} \frac{\alpha}{\pi} Q_l^2 \frac{1}{\beta_l} \left\{ \left[1 + \left(1 - \frac{2m_l^2}{s} \right) J_l \right] \ln \left(\frac{4\omega^2}{\lambda} \right) \right. \\
&\quad + J_l + \left(1 - \frac{2m_l^2}{s} \right) \left[\frac{1}{2} J_l^2 + 2 \ln \left(-\frac{2\beta}{\beta_l^+} \right) J_l \right. \\
&\quad \left. \left. + 2\text{Li}_2 \left(\frac{\beta_l^-}{\beta_l^+} \right) + \frac{\pi^2}{3} \right] \right\},
\end{aligned}$$

where $L_e = \ln(m_e^2/s)$, $\beta_l^\pm = 1 \pm \beta_l$, $J_l = \ln(\beta_l^-)/\beta_l^+$, $d_l = m_l^2 - I$, $I = t, u$.

The cross section for the hard photon bremsstrahlung

$$\begin{aligned}
e^+(p_1, \chi_1) + e^-(p_2, \chi_2) &= l^-(p_3, \chi_3) + l^+(p_4, \chi_4) \\
&\quad + \gamma(p_5, \chi_5)
\end{aligned} \tag{6}$$

is given by the expression

$$\frac{d\sigma_{\chi_1\chi_2}^{\text{hard}}}{ds'd \cos\theta_4 d\phi_4 d \cos\theta_5} = \alpha^3 \frac{s - s'}{32\pi s^2} \frac{\beta_l'}{\beta_e} |\mathcal{H}_{\chi_1\chi_2}^{\text{hard}}|^2, \tag{7}$$

where $s' = (p_3 + p_4)^2$, $\beta_l' = \sqrt{1 - 4m_l^2/s'}$, and

$$|\mathcal{H}_{\chi_1\chi_2}^{\text{hard}}|^2 = \sum_{\chi_3\chi_4\chi_5} |\mathcal{H}_{\chi_1\chi_2\chi_3\chi_4\chi_5}^{\text{hard}}|^2. \tag{8}$$

Here θ_5 is the angle between 3-momenta of the photon and positron, θ_4 is the angle between 3-momenta of the antimuon μ^+ and photon in the rest frame of (l^-l^+) compound, and ϕ_4 is the azimuthal angle of the μ^+ in the rest frame of (l^-l^+) compound.

A. Covariant amplitude for the Born and virtual parts

The covariant one-loop amplitude corresponds to the result of the straightforward standard calculation by means of the SANC programs and procedures of *all* diagrams

contributing to a given process at the tree (Born) and one-loop levels. It is represented in a certain basis made of strings of Dirac matrices and/or external momenta (structures) contracted with polarization vectors of gauge bosons, if any. The amplitude also contains kinematic factors and coupling constants and is parametrized by a certain number of form factors (FFs), which we denote by \mathcal{F} , in general with an index labeling the corresponding structure. The number of FFs is equal to the number of structures.

For processes with nonzero tree-level amplitudes, the FFs have the form

$$\mathcal{F} = 1 + k\tilde{\mathcal{F}}, \tag{9}$$

where “1” is due to the Born level and the term $\tilde{\mathcal{F}}$ with the factor $k = g^2/16\pi^2$ is due to the one-loop level. After squaring the amplitude, we neglect terms proportional to k^2 .

Neglecting the masses of the initial particles, the covariant one-loop amplitude of the $e^+e^- \rightarrow l^-l^+$ process can be parametrized by six FFs. If the initial-state masses were not ignored, we would have ten structures with ten scalar form factors and ten independent helicity amplitudes.

We work in the so-called *LQD* basis, which naturally arises if the final-state fermion masses are not ignored. Six form factors $\mathcal{F}_{LL,QL,LQ,QQ,LD,QD}(s, t, u)$ correspond to six Dirac structures. They are labeled according to their structures. A common expression for this CA in terms of \mathcal{F}_{ij} was presented in [50]. We recall it here to introduce the notation; \mathcal{A}_γ is also described by a *QQ* structure; it is separated out for convenience,

$$\begin{aligned}
\mathcal{A}_\gamma(s) &= ie^2 \frac{Q_e Q_l}{s} \text{Str}_{QQ} \mathcal{F}_\gamma, \\
\mathcal{A}_Z(s) &= ie^2 \frac{\chi_Z(s)}{s} [I_e^{(3)}(I_l^{(3)} \text{Str}_{LL} \mathcal{F}_{LL} + \delta_l \text{Str}_{LQ} \mathcal{F}_{LQ}) \\
&\quad + \delta_e(I_l^{(3)} \text{Str}_{QL} \mathcal{F}_{QL} + \delta_l \text{Str}_{QQ} \mathcal{F}_{QQ}) \\
&\quad + I_l^{(3)}(I_e^{(3)} \text{Str}_{LD} \mathcal{F}_{LD} + \delta_e \text{Str}_{QD} \mathcal{F}_{QD})].
\end{aligned} \tag{10}$$

We use the following notation for the structures:

$$\begin{aligned}
\text{Str}_{LL} &= \gamma_\mu(1 + \gamma_5) \otimes \gamma_\mu(1 + \gamma_5), \\
\text{Str}_{QL} &= \gamma_\mu \otimes \gamma_\mu(1 + \gamma_5), \\
\text{Str}_{LQ} &= \gamma_\mu(1 + \gamma_5) \otimes \gamma_\mu, \\
\text{Str}_{QQ} &= \gamma_\mu \otimes \gamma_\mu, \\
\text{Str}_{LD} &= \gamma_\mu(1 + \gamma_5) \otimes (-im_l D_\mu), \\
\text{Str}_{QD} &= \gamma_\mu \otimes (-im_l D_\mu),
\end{aligned}$$

where the symbol $\gamma_\mu \otimes \gamma_\mu$ denotes the shorthand expression

$$\gamma_\mu \otimes \gamma_\nu = \bar{v}(p_1)\gamma_\mu u(p_2)\bar{u}(p_3)\gamma_\nu v(p_4) \quad (11)$$

and

$$D_\mu = (p_4 - p_3)_\mu. \quad (12)$$

Here and below $\chi_Z(s)$ is the Z/γ propagator ratio,

$$\chi_Z(s) = \frac{1}{4s_W^2 c_W^2} \frac{s}{s - M_Z^2 + iM_Z\Gamma_Z}. \quad (13)$$

We also use the coupling constants

$$Q_f, \quad I_f^{(3)}, \quad \sigma_f = v_f + a_f, \quad \delta_f = v_f - a_f, \\ s_W = \frac{e}{g}, \quad c_W = \frac{M_W}{M_Z}.$$

For more details, see [50].

B. Helicity amplitude for Born and virtual parts

As was stated, we have six nonvanishing HAs. They depend on kinematic variables, coupling constants, and six scalar form factors,

$$\mathcal{H}_{-+-+} = -c_+(Q_e Q_l \mathcal{F}_\gamma \\ + \chi_Z(s)\delta_e[\beta_l^- I_l^{(3)} \mathcal{F}_{QL} + \delta_l \mathcal{F}_{QQ}]), \quad (14)$$

$$\mathcal{H}_{-+--} = \frac{2m_l}{\sqrt{s}} \sin \vartheta_l \left(Q_e Q_l \mathcal{F}_\gamma \\ + \chi_Z(s)\delta_e \left[I_l^{(3)} \mathcal{F}_{QL} + \delta_l \mathcal{F}_{QQ} + \frac{s}{2} \beta_l^2 I_l^{(3)} \mathcal{F}_{QD} \right] \right), \quad (15)$$

$$\mathcal{H}_{+-++} = -\frac{2m_l}{\sqrt{s}} \sin \vartheta_l \left(Q_e Q_l \mathcal{F}_\gamma \\ + \chi_Z(s) \left[2I_e^{(3)} (I_l^{(3)} \mathcal{F}_{LL} + \delta_l \mathcal{F}_{LQ}) + \delta_e I_l^{(3)} \mathcal{F}_{QL} \\ + \delta_e \delta_l \mathcal{F}_{QQ} + \frac{s}{2} \beta_l^2 I_l^{(3)} (2I_e^{(3)} \mathcal{F}_{LD} + \delta_e \mathcal{F}_{QD}) \right] \right), \quad (16)$$

$$\mathcal{H}_{+--+} = -c_+(Q_e Q_l \mathcal{F}_\gamma \\ + \chi_Z(s)[\beta_l^+ I_l^{(3)} (2I_e^{(3)} \mathcal{F}_{LL} + \delta_e \mathcal{F}_{QL}) \\ + \delta_l (2I_e^{(3)} \mathcal{F}_{LQ} + \delta_e \mathcal{F}_{QQ})]). \quad (17)$$

The expression for the amplitude \mathcal{H}_{-+++} (\mathcal{H}_{+--+}) can be obtained from the expression for \mathcal{H}_{-+-+} (\mathcal{H}_{+--+}) by replacing $c_+ \rightarrow c_-$, $\beta_l^- \rightarrow \beta_l^+$.

Helicity indices denote the signs of the fermion spin projections to their momenta p_1, p_2, p_3, p_4 , respectively, where

$$c_\pm = 1 \pm \cos \vartheta_l,$$

and the scattering angle ϑ_l is related to the Mandelstam invariants t, u ,

$$t = m_l^2 - \frac{s}{2}(1 - \beta_l \cos \vartheta_l),$$

$$u = m_l^2 - \frac{s}{2}(1 + \beta_l \cos \vartheta_l).$$

Though we have expressions for the helicity amplitudes, which take into account the initial particle masses, in Eqs. (14)–(17) they are omitted. The presence of the electron masses gives additional terms proportional to the $2m_e/\sqrt{s}$ factor which is equal to 10^{-5} at the Z peak energy and can be considered insignificant in the present calculations.

In order to get helicity amplitudes for the Born level, one should set $F_{\gamma,LL,LQ,QL,QQ} = 1$ and $F_{LD,QD} = 0$.

C. Helicity amplitudes for hard photon bremsstrahlung

We present the HAs for $e^+e^-l^+l^-\gamma \rightarrow 0$ ($\sum p_i = 0$) process at any s, t , or u channel, where 0 stands for *vacuum*, and all masses are not neglected.

The full expression for the photon bremsstrahlung amplitude can be divided into two terms,

$$A_{\dots\chi_i\dots} = 2\sqrt{2}(Q_e A_{\dots\chi_i\dots}^e + Q_l A_{\dots\chi_i\dots}^l). \quad (18)$$

Each term corresponds to a gauge-invariant diagram subset: A^e is the amplitude for radiation from the electron line (ISR) and A^l —for radiation from the final lepton line (FSR).

There exists a crossing symmetry relation between them,

$$A_{\chi_1\chi_2\chi_3\chi_4\chi_5}^l(p_1, p_2, p_3, p_4, p_5) \\ = A_{\chi_3\chi_4\chi_1\chi_2\chi_5}^e(p_3, p_4, p_1, p_2, p_5) \quad \text{and} \quad m_e \leftrightarrow m_l. \quad (19)$$

Explicitly, gauge-invariant form of the amplitude is obtained,

$$\sqrt{2}A_{\chi_1\chi_2\chi_3\chi_4\chi_5}^e = \frac{\text{Tr}[\not{p}_1 \not{p}_2 \mathbf{F}_5]}{z_1 z_2} \bar{v}_1 \not{\epsilon}_{34} u_2 \\ - \frac{\bar{v}_1 \mathbf{F}_5 \not{\epsilon}_{34} u_2}{z_1} - \frac{\bar{v}_1 \not{\epsilon}_{34} \mathbf{F}_5 u_2}{z_2}, \quad (20)$$

with abbreviations $z_i = 2p_i \cdot p_5$, $u_i \equiv u^{i}(p_i)$, etc.

The polarization vector of a real photon appears only in the combination $\mathbf{F}_5 = p_5^\mu \epsilon_5^\nu \sigma_{\mu\nu}$. This is the familiar Maxwell bivector, which is gauge invariant. We introduce also abbreviations for the following combinations of propagators and couplings constants:

$$\not{\epsilon}_{34} = \frac{1}{2} \sum_{a,b=\pm 1} \mathcal{D}^{ab} (\bar{v}_3 \gamma^\mu \gamma_b u_4) \gamma_\mu \gamma_a, \quad (21)$$

$$\mathcal{D}^{ab} = \frac{Q_e Q_l}{s'} + \frac{g_e^a g_l^b}{s' - M_Z^2 + iM_Z \Gamma_Z},$$

where g_l^\pm are the chiral couplings of the leptons l to the vector boson Z .

We work in the chiral representation of gamma matrices and exploit Weyl spinors. Our notation is consistent with [63,64]. Below we use the following denotation for the Dirac spinor decomposition into the Weyl one:

$$\not{p} = \begin{pmatrix} & P_{A\dot{B}} \\ P^{\dot{A}B} & \end{pmatrix} = \begin{pmatrix} & \not{p} \\ \hat{p} & \end{pmatrix}, \quad u = \begin{pmatrix} u_A \\ u^{\dot{A}} \end{pmatrix} = \begin{pmatrix} |u\rangle \\ |u] \end{pmatrix},$$

$$\bar{u} = (\bar{u}^A, \bar{u}_{\dot{A}}) = (\langle \bar{u}|, [\bar{u}|),$$

$$\mathbf{F} = \begin{pmatrix} \mathbf{F}_A^B & \\ & \mathbf{F}^{\dot{A}\dot{B}} \end{pmatrix} = \begin{pmatrix} \check{\mathbf{F}} & \\ & \hat{\mathbf{F}} \end{pmatrix}. \quad (22)$$

Application of the Fiertz identities to the Pauli matrices yields

$$\hat{e}_{34} = |\bar{v}_3\rangle \mathcal{D}^{++} \langle u_4| + |u_4\rangle \mathcal{D}^{+-} \langle \bar{v}_3|,$$

$$\check{e}_{34} = |u_4\rangle \mathcal{D}^{-+} [\bar{v}_3| + [\bar{v}_3] \mathcal{D}^{--} [u_4|. \quad (23)$$

The HAs are not Lorentz-invariant objects (they change with boosts transverse to a momentum ray) and thus rudimentally depend on an experimental setup. However, one expects that all physical content of a reaction should depend only on a relative configuration of particles by analogy with the rigid body dynamics in a rotating reference frame. This type of description usually appears to be most economic one.

In order to factor out all information related to a configuration of experiment, we must build a spin basis in terms of problems momenta. Our investigations show that one of the most economic choices is to put the polarization vector of fermion n_i with $i = 1 \dots 4$ into the same two-plane with its momentum p_i and momentum of photon p_5 . Each two-plane contains two lightlike vectors: photon momentum and the other one denoted by k_i . Explicit expressions for k_i can be found in [65].

Then, in the photon basis, we have

$$|u_i^+\rangle = |v_i^-\rangle = |\bar{u}_i^-\rangle = |\bar{v}_i^+\rangle = |k_i\rangle \equiv |i\rangle,$$

$$|u_i^-\rangle = |v_i^+\rangle = |\bar{u}_i^+\rangle = |\bar{v}_i^-\rangle = |k_i\rangle \equiv |i],$$

$$|u_i^+\rangle = -|v_i^-\rangle = -|\bar{u}_i^-\rangle = |\bar{v}_i^+\rangle = -|5\rangle \zeta_i^*,$$

$$|u_i^-\rangle = -|v_i^+\rangle = -|\bar{u}_i^+\rangle = |\bar{v}_i^-\rangle = |5] \zeta_i, \quad (24)$$

with $\zeta_i = m_i / \langle i|5\rangle$, where we identify $k_5 \equiv p_5$.

Maxwell bivector has a factorized form in spinor notation $\check{\mathbf{F}}_5^+ = \sqrt{2}|5\rangle\langle 5|$, $\hat{\mathbf{F}}_5^- = \sqrt{2}|5][5|$, $\check{\mathbf{F}}_5^- = \hat{\mathbf{F}}_5^+ = 0$, which allows us to organize the amplitude in terms of blocks,

$$A_{\chi_1 \chi_2 \chi_3 \chi_4 \chi_5}^e = \mathcal{S}_{\chi_5} \mathcal{B}_{\chi_1 \chi_2 \chi_3 \chi_4} - C_{\chi_1 \chi_5}^1 \mathcal{G}_{\chi_2 \chi_3 \chi_4 \chi_5}^2 - C_{\chi_2 \chi_5}^2 \mathcal{G}_{\chi_1 \chi_3 \chi_4 \chi_5}^1, \quad (25)$$

where

$$\mathcal{B}_{\chi_1 \chi_2 \chi_3 \chi_4} = [\bar{v}_1 | \hat{e}_{34} | u_2\rangle + [\bar{v}_1 | \check{e}_{34} | u_2], \quad (26)$$

$$\mathcal{G}_{\chi_1 \chi_3 \chi_4 \pm}^1 = \begin{bmatrix} [\bar{v}_1 | \hat{e}_{34} | 5] \\ \langle \bar{v}_1 | \check{e}_{34} | 5] \end{bmatrix}, \quad \mathcal{G}_{\chi_2 \chi_3 \chi_4 \pm}^2 = \begin{bmatrix} \langle 5 | \check{e}_{34} | u_2\rangle \\ [5 | \hat{e}_{34} | u_2] \end{bmatrix},$$

$$\mathcal{S}_{\chi_5} = - \begin{bmatrix} [1|2] \\ [1|5][2|5] \end{bmatrix}, \quad \langle 1|2\rangle, \quad \langle 1|5\rangle\langle 2|5\rangle,$$

$$C_{\chi_1 \chi_5}^1 = \begin{bmatrix} [5|1] \\ \langle 5|1] \end{bmatrix}^{-1}, \quad C_{\chi_2 \chi_5}^2 = \begin{bmatrix} [2|5] \\ \langle 2|5] \end{bmatrix}^{-1}.$$

We are going to evaluate the amplitude only for positive photon helicity, because the case of negative one can be easily obtained with CP symmetry,

$$A_{\chi_1 \chi_2 \chi_3 \chi_4} = -\chi_1 \chi_2 \chi_3 \chi_4 A_{-\chi_1 -\chi_2 -\chi_3 -\chi_4}^*, \quad (27)$$

with “+” \leftrightarrow “-” in \mathcal{D}^{ab} .

Below we give all amplitudes with positive photon helicity,

$$A_{e-----}^e = -\mathcal{S}_+ \langle 4|5\rangle (\mathcal{D}^{++} [3|1] \zeta_2 + \mathcal{D}^{-+} [3|2] \zeta_1),$$

$$A_{e-----}^e = -\mathcal{S}_+ \langle 3|5\rangle (\mathcal{D}^{+-} [4|1] \zeta_2 + \mathcal{D}^{--} [4|2] \zeta_1),$$

$$A_{e-+----}^e = \mathcal{S}_+ \langle 2|5\rangle (\mathcal{D}^{++} [3|1] \zeta_4 + \mathcal{D}^{+-} [4|1] \zeta_3),$$

$$A_{e+----}^e = \mathcal{S}_+ \langle 1|5\rangle (\mathcal{D}^{-+} [3|2] \zeta_4 + \mathcal{D}^{--} [4|2] \zeta_3),$$

$$A_{e-----}^e = \mathcal{S}_+ [5|1] (\mathcal{D}^{+-} \langle 3|5\rangle \zeta_2 \zeta_4^* + \mathcal{D}^{++} \langle 4|5\rangle \zeta_2 \zeta_3^*)$$

$$+ \mathcal{S}_+ [5|2] (\mathcal{D}^{--} \langle 3|5\rangle \zeta_1 \zeta_4^* + \mathcal{D}^{-+} \langle 4|5\rangle \zeta_1 \zeta_3^*),$$

$$A_{e+----}^e = \mathcal{S}_+ \langle 1|5\rangle (\mathcal{D}^{-+} [5|3] \zeta_2^* \zeta_4 + \mathcal{D}^{--} [5|4] \zeta_2^* \zeta_3)$$

$$+ \mathcal{S}_+ \langle 2|5\rangle (\mathcal{D}^{++} [5|3] \zeta_1^* \zeta_4 + \mathcal{D}^{+-} [5|4] \zeta_1^* \zeta_3),$$

$$A_{e-+----}^e = \mathcal{S}_+ (\mathcal{D}^{++} [3|1] \langle 2|4\rangle - \mathcal{D}^{-+} \langle 4|5\rangle [5|3] \zeta_1 \zeta_2^*$$

$$- \mathcal{D}^{+-} \langle 2|5\rangle [5|1] \zeta_3 \zeta_4^*) + C_{++}^2 \mathcal{D}^{++} [3|1] \langle 4|5\rangle,$$

$$A_{e-+----}^e = \mathcal{S}_+ (\mathcal{D}^{+-} [4|1] \langle 2|3\rangle - \mathcal{D}^{--} \langle 3|5\rangle [5|4] \zeta_1 \zeta_2^*$$

$$- \mathcal{D}^{++} \langle 2|5\rangle [5|1] \zeta_3^* \zeta_4) + C_{++}^2 \mathcal{D}^{+-} [4|1] \langle 4|5\rangle,$$

$$A_{e+----}^e = \mathcal{S}_+ (\mathcal{D}^{-+} [3|2] \langle 1|4\rangle - \mathcal{D}^{++} \langle 4|5\rangle [5|3] \zeta_1^* \zeta_2$$

$$- \mathcal{D}^{--} \langle 1|5\rangle [5|2] \zeta_3 \zeta_4^*) + C_{++}^1 \mathcal{D}^{-+} [3|2] \langle 4|5\rangle,$$

$$A_{e+----}^e = \mathcal{S}_+ (\mathcal{D}^{--} [4|2] \langle 1|3\rangle - \mathcal{D}^{+-} \langle 3|5\rangle [5|4] \zeta_1^* \zeta_2$$

$$- \mathcal{D}^{-+} \langle 1|5\rangle [5|2] \zeta_3^* \zeta_4) + C_{++}^1 \mathcal{D}^{--} [4|2] \langle 3|5\rangle,$$

$$A_{e-----}^e = -\mathcal{S}_+ [5|1] (\mathcal{D}^{+-} \langle 2|3\rangle \zeta_4^* + \mathcal{D}^{++} \langle 2|4\rangle \zeta_3^*)$$

$$- C_{++}^2 [5|1] (\mathcal{D}^{+-} \langle 3|5\rangle \zeta_4^* + \mathcal{D}^{++} \langle 4|5\rangle \zeta_3^*),$$

$$\begin{aligned}
A^e_{-++++} &= -\mathcal{S}_+[5|2](\mathcal{D}^{--}\langle 1|3\rangle\zeta_4^* + \mathcal{D}^{-+}\langle 1|4\rangle\zeta_3^*) \\
&\quad - \mathcal{C}_{++}^2[5|2](\mathcal{D}^{--}\langle 3|5\rangle\zeta_4^* + \mathcal{D}^{-+}\langle 4|5\rangle\zeta_3^*), \\
A^e_{++++} &= \mathcal{S}_+[5|3](\mathcal{D}^{-+}\langle 1|4\rangle\zeta_2^* + \mathcal{D}^{++}\langle 2|4\rangle\zeta_1^*) \\
&\quad + \langle 4|5\rangle[5|3](\mathcal{C}_{++}^1\mathcal{D}^{-+}\zeta_2^* + \mathcal{C}_{++}^2\mathcal{D}^{++}\zeta_1^*), \\
A^e_{++++} &= \mathcal{S}_+[5|4](\mathcal{D}^{--}\langle 1|3\rangle\zeta_2^* + \mathcal{D}^{-+}\langle 2|3\rangle\zeta_1^*) \\
&\quad + \langle 3|5\rangle[5|4](\mathcal{C}_{++}^1\mathcal{D}^{--}\zeta_2^* + \mathcal{C}_{++}^2\mathcal{D}^{-+}\zeta_1^*), \\
A^e_{++++} &= A^e_{-----} = 0.
\end{aligned}$$

To obtain HA \mathcal{H} with definite helicity, the basis-transformation matrices $C_{\xi_i}^{\chi_i}$ should be applied independently for each index χ of external particles whose polarization is not averaged,

$$\mathcal{H}_{\dots\xi_i\dots} = C_{\xi_1}^{\chi_1} \dots C_{\xi_4}^{\chi_4} A_{\dots\chi_i\dots}. \quad (28)$$

Explicit expressions for the matrices C can be found in [66] and for our special case in [65]. Geometrically, they realize the Wigner rotation of the spin axis [67,68].

III. NUMERICAL RESULTS AND COMPARISONS

In this section, we show numerical results for EW RC to $e^+e^- \rightarrow \mu^-\mu^+$ scattering obtained by means of the SANC system. Comparison of our results for specific contributions at the tree level with CalcHEP [57] and WHIZARD [58–61] is given. Numerical results are completed by estimating the polarization effect and evaluating angular and energy distributions at the one-loop level.

We used the following set of input parameters:

$$\begin{aligned}
\alpha^{-1}(0) &= 137.03599976, \\
M_W &= 80.45150 \text{ GeV}, & M_Z &= 91.1867 \text{ GeV}, \\
\Gamma_Z &= 2.49977 \text{ GeV}, & m_e &= 0.51099907 \text{ MeV}, \\
m_\mu &= 0.105658389 \text{ GeV}, & m_\tau &= 1.77705 \text{ GeV}, \\
m_d &= 0.083 \text{ GeV}, & m_s &= 0.215 \text{ GeV}, \\
m_b &= 4.7 \text{ GeV}, & m_u &= 0.062 \text{ GeV}, \\
m_c &= 1.5 \text{ GeV}, & m_t &= 173.8 \text{ GeV}. \quad (29)
\end{aligned}$$

The $\alpha(0)$ and G_μ EW schemes are used in calculations. All the results are obtained for the c.m. energies $\sqrt{s} = 250, 500, \text{ and } 1000 \text{ GeV}$ and for the following magnitudes of the electron (P_{e^-}) and positron (P_{e^+}) beam polarizations [7,15,51]:

$$\begin{aligned}
(P_{e^-}, P_{e^+}) &= (0, 0), (-0.8, 0), (-0.8, 0.3), (0.8, 0), (0.8, -0.3). \\
&\quad (30)
\end{aligned}$$

A. Comparison with other codes

1. Triple comparison of the Born and hard photon bremsstrahlung cross sections

First of all, we have compared the numerical results for the polarized Born and hard photon bremsstrahlung cross section with the ones obtained with the help of the CalcHEP and WHIZARD. The agreement for the Born cross section was found to be excellent.

Since the integration of the hard photon bremsstrahlung cross section without any angular cuts is an unstable task, additional efforts have been made to compare the results: the CALCHEP code was recompiled with quadruple precision and the ‘‘BreitWigner range parameter’’ was adjusted; WHIZARD code was recompiled with the support of extended precision numbers, and phase-space setup was tuned to work better without any cuts.

Table I gives the triple tuned comparison between the SANC (S), CalcHEP (C), and WHIZARD (W) of the hard photon bremsstrahlung (6) cross section calculations.

The results are given within the $\alpha(0)$ scheme for c.m. energies $\sqrt{s} = 250, 500, \text{ and } 1000 \text{ GeV}$, $\omega = 10^{-4}$, and the fixed 100% polarized initial states in the total phase space.

The comparison demonstrates very good (within four to five digits) agreement with the above-mentioned codes.

2. Comparison of virtual and soft photon bremsstrahlung contributions

We have obtained very good agreement (six significant digits) in the comparison of the SANC and AITALC-1.4 [62] results for the unpolarized differential Born cross section and for the sum of virtual and soft photon bremsstrahlung contributions. The comparison was carried out for different values of the scattering angles ($\cos\vartheta$: from -0.9 up to $+0.9999$).

TABLE I. The triple tuned comparison between the SANC (S), CalcHEP (C), and WHIZARD (W) of the hard photon bremsstrahlung (6) cross section calculations.

P_{e^-}, P_{e^+}	-1, -1	1, -1	-1, 1	1, 1
$\sigma_{e^+e^-}^{\text{hard}}, \text{ fb}, \sqrt{s} = 250, \text{ GeV}$				
S	169.0(1)	8802(1)	11263(1)	169.0(1)
C	168.9(1)	8801(1)	11262(1)	169.0(1)
W	169.0(1)	8802(1)	11263(1)	169.0(1)
$\sigma_{e^+e^-}^{\text{hard}}, \text{ fb}, \sqrt{s} = 500, \text{ GeV}$				
S	47.38(1)	2314(1)	2899(1)	47.38(1)
C	47.38(1)	2314(1)	2898(1)	47.38(1)
W	47.38(1)	2314(1)	2899(1)	47.38(1)
$\sigma_{e^+e^-}^{\text{hard}}, \text{ fb}, \sqrt{s} = 1000, \text{ GeV}$				
S	12.65(1)	624.7(1)	778.8(1)	12.65(1)
C	12.65(1)	624.7(1)	778.7(1)	12.64(1)
W	12.65(1)	624.7(1)	778.8(1)	12.65(1)

TABLE II. Born cross sections, weak contribution (weak) and complete one-loop contributions (EW), and relative corrections δ (%) for the c.m. energy $\sqrt{s} = 250$ GeV and the set (30) of the polarization degree of the initial particles in the $\alpha(0)$ and G_μ EW schemes.

P_{e^+}, P_{e^-}	0, 0	0, -0.8	0.3, -0.8	0, 0.8	-0.3, 0.8
$\sigma_{\alpha(0)}^{\text{Born}}$, pb	1.6537(1)	1.8040(1)	2.2572(1)	1.5034(1)	1.8440(1)
$\sigma_{G_\mu}^{\text{Born}}$, pb	1.7611(1)	1.9212(1)	2.4039(1)	1.6011(1)	1.9638(1)
$\sigma_{\alpha(0)}^{\text{weak}}$, pb	1.8360(1)	1.9447(1)	2.4261(1)	1.7273(1)	2.1271(1)
δ , %	11.03(1)	7.81(1)	7.49(1)	14.89(1)	15.36(1)
$\sigma_{G_\mu}^{\text{weak}}$, pb	1.8547(1)	1.9614(1)	2.4466(1)	1.7480(1)	2.1532(1)
δ , %	5.31(1)	2.10(1)	1.78(1)	9.18(1)	9.64(1)
$\sigma_{\alpha(0)}^{\text{EW}}$, pb	4.534(1)	4.923(1)	6.115(1)	4.145(1)	5.047(1)
δ , %	174.2(1)	172.9(1)	170.9(1)	175.7(1)	173.7(1)
$\sigma_{G_\mu}^{\text{EW}}$, pb	4.728(1)	5.132(1)	6.376(1)	4.323(1)	5.263(1)
δ , %	168.5(1)	167.1(1)	165.2(1)	170.0(1)	168.0(1)

B. Born, one-loop cross sections and relative corrections

1. Energy dependence

In Tables II–IV, the results of the Born cross sections, weak contribution (weak), and complete one-loop contributions (EW), as well as the relative corrections δ (%) for the c.m. energies $\sqrt{s} = 250, 500, 1000$ GeV, and the set (30) of the polarization degree of the initial particles in the $\alpha(0)$ and G_μ EW schemes are presented. The results were obtained without any angular cuts.

The relative correction δ (in %) is defined as

$$\delta = \frac{\sigma^{\text{one-loop}}(P_{e^-}, P_{e^+})}{\sigma^{\text{Born}}(P_{e^-}, P_{e^+})} - 1. \quad (31)$$

As is seen from the tables, the corrections for all considered c.m. energies, EW schemes, and degrees of

polarization are positive, rather large and equal to about 170%–175% for the c.m. energy $\sqrt{s} = 250$ GeV, about 182%–186% for the c.m. energy $\sqrt{s} = 500$ GeV, and about 200%–204% for the c.m. energy $\sqrt{s} = 1000$ GeV in the $\alpha(0)$ EW scheme. The calculations in the G_μ scheme reduce RCs by about 5%–6%.

The main impact on one-loop corrections is due to the QED contributions. It can be described by large logarithms of the radiating particle masses ($\ln s/m_l^2$) appearing for collinear photons. The contribution of the collinear photons is clearly seen from Fig. 1, where a rapid increase of the cross section at small angles of the final muon ($|\cos \vartheta_\mu| \approx 1$) is observed. The real-life experimental angular cuts can rapidly reduce the QED radiative corrections and the whole cross section.

The degree of the initial particle polarization changes the magnitude of the cross section, the minimal value achieved for unpolarized beams and the maximum (from the set (30)) for the $(P_{e^-}, P_{e^+}) = (0.3, -0.8)$ ones. It can be useful to increase the signal reaction.

2. Angular distributions

In Fig. 1, the unpolarized Born and complete one-loop cross section for c.m. energies $\sqrt{s} = 250, 500, 1000$ GeV are shown for the muon angle. As is seen, the Born distributions are rather smooth, while the EW one-loop RCs have large values at small angles. As it was mentioned above, this is due to the collinear emitted photons. Both distributions are asymmetric.

Since the polarization effects do not change the form of the distributions, only unpolarized cross section is shown. The integrated values of the polarization effects are shown in Tables II–IV.

C. Left-right asymmetry

In Fig. 2, the left-right asymmetry distributions are shown as a function of the muon angle cosine. The A_{LR} is defined in the following form:

TABLE III. The same as in Table II for the c.m. energy $\sqrt{s} = 500$ GeV.

P_{e^+}, P_{e^-}	0, 0	0, -0.8	0.3, -0.8	0, 0.8	-0.3, 0.8
$\sigma_{\alpha(0)}^{\text{Born}}$, pb	0.40084(1)	0.43351(1)	0.54196(1)	0.36820(1)	0.45215(1)
$\sigma_{G_\mu}^{\text{Born}}$, pb	0.42689(1)	0.46167(1)	0.57717(1)	0.39211(1)	0.48152(1)
$\sigma_{\alpha(0)}^{\text{weak}}$, pb	0.44633(1)	0.46766(1)	0.58278(1)	0.42501(1)	0.52413(1)
δ , %	11.35(1)	7.88(1)	7.53(1)	15.43(1)	15.92(1)
$\sigma_{G_\mu}^{\text{weak}}$, pb	0.45095(1)	0.47168(1)	0.58768(1)	0.43022(1)	0.53067(1)
δ , %	5.64(1)	2.17(1)	1.82(1)	9.72(1)	10.21(1)
$\sigma_{\alpha(0)}^{\text{EW}}$, pb	1.145(1)	1.233(1)	1.531(1)	1.056(1)	1.286(1)
δ , %	185.7(1)	184.5(1)	182.4(1)	186.8(1)	184.5(1)
$\sigma_{G_\mu}^{\text{EW}}$, pb	1.195(1)	1.287(1)	1.597(1)	1.102(1)	1.342(1)
δ , %	180.0(1)	178.8(1)	176.7(1)	181.1(1)	178.8(1)

TABLE IV. The same as in Table II for the c.m. energy $\sqrt{s} = 1000$ GeV.

P_{e^+}, P_{e^-}	0, 0	0, -0.8	0.3, -0.8	0, 0.8	-0.3, 0.8
$\sigma_{\alpha(0)}^{\text{Born}}$, pb	0.099570(1)	0.107474(1)	0.134335(1)	0.091666(1)	0.112599(1)
$\sigma_{G_\mu}^{\text{Born}}$, pb	0.106038(1)	0.114455(1)	0.143061(1)	0.097620(1)	0.119913(1)
$\sigma_{\alpha(0)}^{\text{weak}}$, pb	0.11017(1)	0.11422(1)	0.14218(1)	0.10611(1)	0.13103(1)
δ , %	10.64(1)	6.28(1)	5.85(1)	15.8(1)	16.4(1)
$\sigma_{G_\mu}^{\text{weak}}$, pb	0.11127(1)	0.11511(1)	0.14325(1)	0.10743(1)	0.13269(1)
δ , %	4.93(1)	0.57(1)	0.13(1)	10.05(1)	10.66(1)
$\sigma_{\alpha(0)}^{\text{EW}}$, pb	0.3003(1)	0.3223(1)	0.3997(1)	0.2782(1)	0.3392(1)
δ , %	201.6(1)	199.9(1)	197.5(1)	203.5(1)	201.2(1)
$\sigma_{G_\mu}^{\text{EW}}$, pb	0.3137(1)	0.3367(1)	0.4176(1)	0.2907(1)	0.3543(1)
δ , %	195.9(1)	194.2(1)	191.9(1)	197.8(1)	195.5(1)

$$A_{LR} = \frac{\sigma_{LR} - \sigma_{RL}}{\sigma_{LR} + \sigma_{RL}}, \quad (32)$$

where σ_{LR} and σ_{RL} are the cross sections for 100% polarized electron-positron $e_L^- e_R^+$ and $e_R^- e_L^+$ initial states.

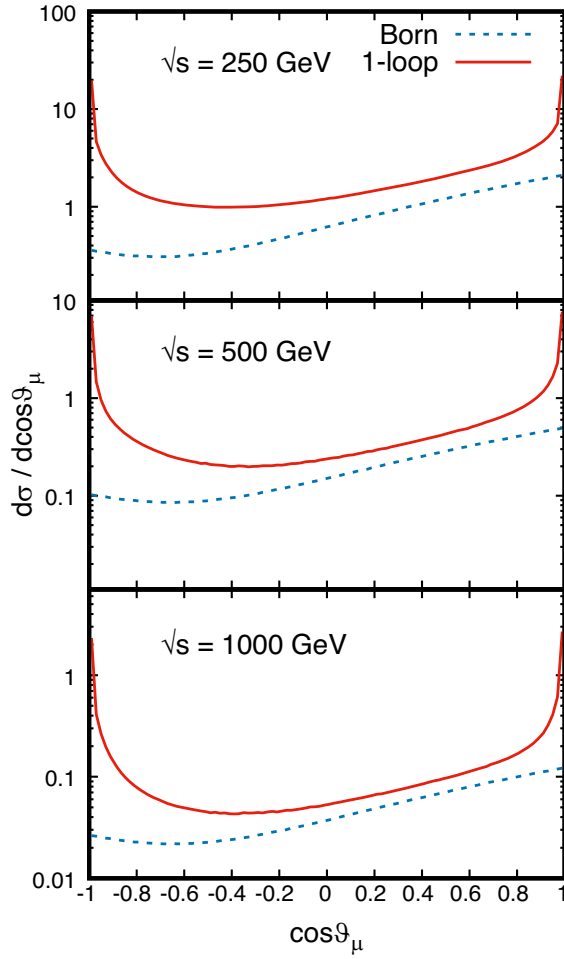


FIG. 1. The Born (dashed line) and one-loop (solid line) differential cross sections of the $e^+e^- \rightarrow \mu^-\mu^+$ reaction for the c.m. energies $\sqrt{s} = 250, 500, 1000$ GeV.

The A_{LR} asymmetry distributions for the Born and one-loop contribution are shown for three c.m. energies $\sqrt{s} = 250, 500, 1000$ GeV.

One can see that the EW RCs strongly affect the asymmetry. The Born contribution to A_{LR} has a smooth

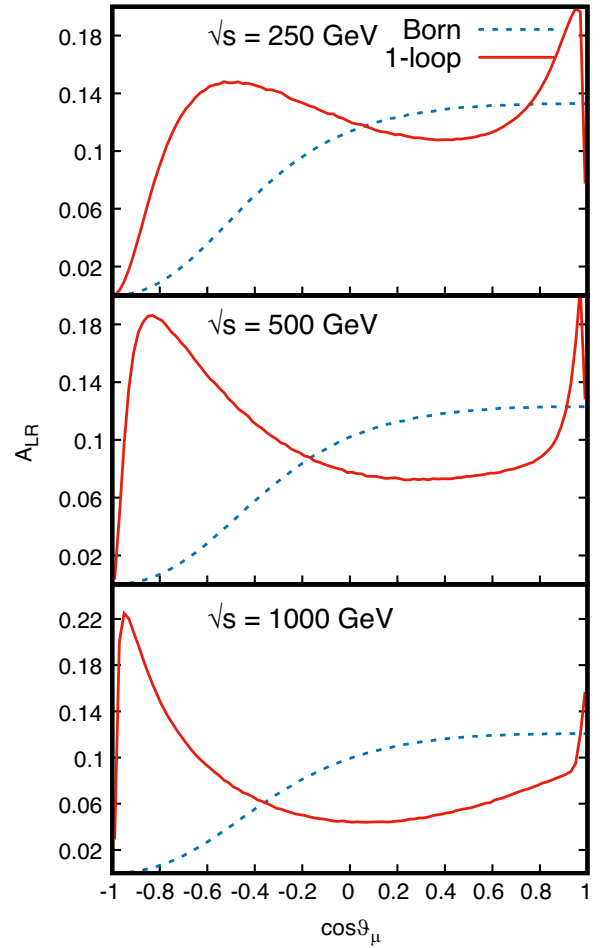


FIG. 2. The dependence of the A_{LR} asymmetry on the muon angle for the Born (dashed line) and one-loop (solid line) contributions for three c.m. energies $\sqrt{s} = 250, 500, 1000$ GeV.

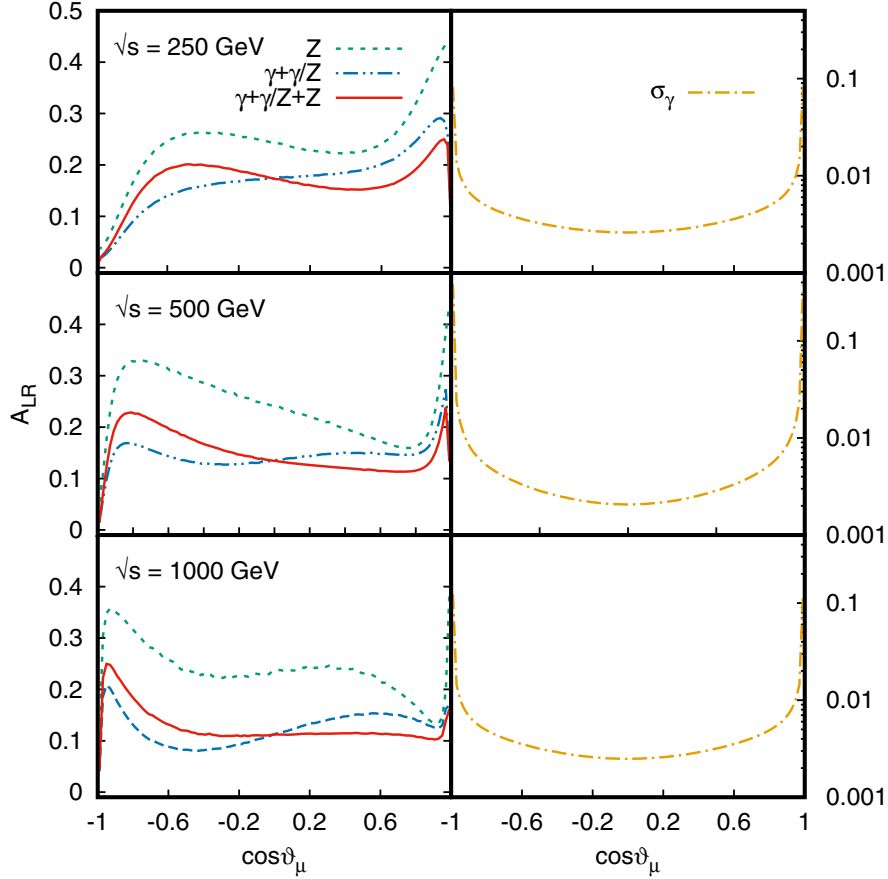


FIG. 3. The contributions of the intermediate Z boson and photon propagators to the A_{LR} asymmetry (ISR part of hard photon bremsstrahlung).

dependence on $\cos \vartheta_\mu$, equals zero at $\cos \vartheta_\mu = -1$, and the value 0.12–0.14 depending on the c.m energy. The one-loop contribution has two maxima: the first at $\cos \vartheta_\mu = 1$ and the other one at $\cos \vartheta_\mu = -0.6$ for $\sqrt{s} = 250$ GeV, $\cos \vartheta_\mu = -0.8$ for $\sqrt{s} = 500$ GeV, and around the $\cos \vartheta_\mu = -1$ for $\sqrt{s} = 1000$ GeV.

The shape of A_{LR} is mainly formed by the radiation of hard photons from the initial electron-positron pair. The left and right peaks of A_{LR} are defined by a specific interplay of the intermediate Z boson and photon propagator contributions (note that the symmetric photon contribution affects only the denominator of A_{LR}). Besides, the interference γ/Z term has an influence on the scale of A_{LR} ; see Fig. 3.

During the LEP era, the A_{LR} asymmetry (as well as A_{FB} , A_{FBLR} and final lepton polarization) calculated at the Z pole was used to measure experimentally $\sin^2 \theta_W$. A comprehensive investigation of the one-loop contribution to the above-mentioned variables in wide c.m. energy region ($\sqrt{s} = 20$ –500 GeV) can be found in [53].

IV. CONCLUSIONS AND OUTLOOK

The theoretical description of $e^+e^- \rightarrow l^+l^-$ scattering taking into account complete one-loop and high-order

radiative corrections is crucial for luminosity monitoring at modern and future e^+e^- colliders. Consideration of beam polarization is a novel requirement for theoretical predictions for e^+e^- collisions at CLIC and ILC energies.

In the paper, we have described the implementation of the complete one-loop EW calculations including the hard photon bremsstrahlung contribution to the SANC framework. It allows one to calculate observables for polarization processes of the lepton pair production.

In this study, the relevant contributions to the cross section are calculated analytically using the helicity amplitudes approach, which allows one to evaluate the contribution of any polarization of the initial and final fermions and then estimated numerically. The helicity amplitudes were used not only for the Born-like parts but also for the hard photon bremsstrahlung contribution taking into account the initial and final masses of radiate particles. The effect of polarization of the initial beams is carefully analyzed for certain states. The angular and energy dependences are also considered.

All contributions to the complete one-loop corrections, i.e., Born, virtual, and real soft and hard photon bremsstrahlung, were obtained using the helicity amplitude approach. The independence of the form factors of the

gauge parameters was tested, and the stability of the result on the variation of the soft-hard separation parameter ω was checked.

The calculated polarized tree-level cross sections for the Born and hard photon bremsstrahlung were compared with the CALCHEP and WHIZARD results and very good (within four to five digits) agreement with the above-mentioned codes was found.

Also, we obtained very good agreement (six significant digits) in comparing the SANC and AITALC-1.4 [62] results for the unpolarized differential Born cross section and for the sum of virtual and soft photon bremsstrahlung contributions.

As a result, the polarization effects are significant and give increase in the cross section at the definite initial degrees of polarization compared to the unpolarized one.

We show that the complete $\mathcal{O}(\alpha)$ electroweak radiative corrections provide a considerable impact on the differential cross section and the left-right asymmetry A_{LR} . Moreover, the corrections themselves are rather sensitive to polarization degrees of the initial beams and depend quite strongly on energy.

Considering the $e^+e^- \rightarrow l^-l^+$ process as one for the purpose of luminometry, one needs to take into account high-order effects, such as leading multiphoton QED logarithms and leading EW and mixed QCD-EW multiloop corrections. It will be implemented in the future.

ACKNOWLEDGMENTS

The reported study was funded by Russian Foundation for Basic Research, Project No. 20-02-00441. We are grateful to Dr. A. Gladyshev and Dr. A. Saprionov for the help in preparation of the paper.

-
- [1] ILC, <https://ilchome.web.cern.ch/>.
- [2] A. Irlles, R. Poschl, F. Richard, and H. Yamamoto, [arXiv:1905.00220](https://arxiv.org/abs/1905.00220).
- [3] A. Arbey *et al.*, *Eur. Phys. J. C* **75**, 371 (2015).
- [4] H. Baer, T. Barklow, K. Fujii, Y. Gao, A. Hoang, S. Kanemura, J. List, H. E. Logan, A. Nomerotski, M. Perelstein *et al.*, [arXiv:1306.6352](https://arxiv.org/abs/1306.6352).
- [5] E. Accomando *et al.* (ECFA/DESY LC Physics Working Group Collaboration), *Phys. Rep.* **299**, 1 (1998).
- [6] E. Accomando *et al.* (CLIC Physics Working Group), [arXiv:hep-ph/0412251](https://arxiv.org/abs/hep-ph/0412251).
- [7] P. Bambade *et al.*, [arXiv:1903.01629](https://arxiv.org/abs/1903.01629).
- [8] FCC-ee, <http://tlep.web.cern.ch>.
- [9] A. Abada *et al.* (FCC Collaboration), *Eur. Phys. J. Spec. Top.* **228**, 1109 (2019).
- [10] A. Abada *et al.* (FCC Collaboration), *Eur. Phys. J. C* **79**, 474 (2019).
- [11] A. Blondel and P. Janot, [arXiv:1912.11871](https://arxiv.org/abs/1912.11871).
- [12] A. Blondel *et al.*, Standard model theory for the FCC-ee Tera-Z stage, in *Mini Workshop on Precision EW and QCD Calculations for the FCC Studies: Methods and Techniques CERN, Geneva, Switzerland, 2018* (CERN, Geneva, 2019), Vol. 3.
- [13] CLIC, <http://clic-study.web.cern.ch>.
- [14] M. J. Boland *et al.* (CLIC, CLICdp Collaboration), [arXiv:1608.07537](https://arxiv.org/abs/1608.07537).
- [15] T. K. Charles *et al.* (CLICdp, CLIC Collaboration), *CERN Yellow Rep. Monogr.* **1802**, 1 (2018).
- [16] CEPC, <http://cepc.ihep.ac.cn>.
- [17] A. Blondel, A. Freitas, J. Gluza, T. Riemann, S. Heinemeyer, S. Jadach, and P. Janot, [arXiv:1901.02648](https://arxiv.org/abs/1901.02648).
- [18] G. Passarino and M. J. G. Veltman, *Nucl. Phys.* **B160**, 151 (1979).
- [19] D. Yu. Bardin, P. K. Khristova, and O. M. Fedorenko, *Nucl. Phys.* **B197**, 1 (1982).
- [20] D. Yu. Bardin, P. K. Khristova, and O. M. Fedorenko, *Nucl. Phys.* **B175**, 435 (1980).
- [21] A. A. Akhundov, D. Yu. Bardin, O. M. Fedorenko, and T. Riemann, *Yad. Fiz.* **42**, 1204 (1985) [*Sov. J. Nucl. Phys.* **42**, 762 (1985)], <https://lib-extopc.kek.jp/preprints/PDF/1985/8504/8504111.pdf>.
- [22] F. A. Berends, G. Burgers, W. Hollik, and W. L. van Neerven, *Phys. Lett. B* **203**, 177 (1988).
- [23] D. Yu. Bardin, M. S. Bilenky, T. Riemann, M. Sachwitz, and H. Vogt, *Comput. Phys. Commun.* **59**, 303 (1990).
- [24] W. F. L. Hollik, *Fortsch. Phys.* **38**, 165 (1990).
- [25] G. Montagna, F. Piccinini, O. Nicrosini, G. Passarino, and R. Pittau, *Comput. Phys. Commun.* **76**, 328 (1993).
- [26] G. Montagna, O. Nicrosini, G. Passarino, and F. Piccinini, *Comput. Phys. Commun.* **93**, 120 (1996).
- [27] G. Montagna, O. Nicrosini, F. Piccinini, and G. Passarino, *Comput. Phys. Commun.* **117**, 278 (1999).
- [28] D. Yu. Bardin, P. Christova, M. Jack, L. Kalinovskaya, A. Olchevski, S. Riemann, and T. Riemann, *Comput. Phys. Commun.* **133**, 229 (2001).
- [29] W. Beenakker, F. A. Berends, and S. C. van der Marck, *Nucl. Phys.* **B349**, 323 (1991).
- [30] W. Beenakker, F. A. Berends, and S. C. van der Marck, *Phys. Lett. B* **251**, 299 (1990).
- [31] D. Yu. Bardin and G. Passarino, *The Standard Model in the Making: Precision Study of the Electroweak Interactions* (Clarendon, Oxford, United Kingdom, 1999), p. 685.
- [32] D. Yu. Bardin, O. M. Fedorenko, and N. M. Shumeiko, *Yad. Fiz.* **32**, 782 (1980) [*Sov. J. Nucl. Phys.* **32**, 403 (1980)], <https://inspirehep.net/files/0ffb82c05847df6f3559-e2b6d2a1fde7>.
- [33] W. Hollik, *Z. Phys. C* **8**, 149 (1981).
- [34] M. Bohm and W. Hollik, *Nucl. Phys.* **B204**, 45 (1982).
- [35] M. Bohm and W. Hollik, *Phys. Lett.* **139B**, 213 (1984).

- [36] T. V. Kukhto and N. M. Shumeiko, *Nucl. Phys.* **B219**, 412 (1983).
- [37] M. W. Grunewald, *Phys. Rep.* **322**, 125 (1999).
- [38] S. Jadach, B. Ward, and Z. Was, *Phys. Lett. B* **449**, 97 (1999).
- [39] S. Jadach, B. Ward, and Z. Was, *Comput. Phys. Commun.* **130**, 260 (2000).
- [40] S. Jadach, B. Ward, and Z. Was, *Phys. Rev. D* **63**, 113009 (2001).
- [41] R. Kleiss and W. Stirling, *Nucl. Phys.* **B262**, 235 (1985).
- [42] D. M. Asner *et al.*, *Int. J. Mod. Phys. A* **24**, 499 (2009).
- [43] D. Bardin, Y. Dydyshka, L. Kalinovskaya, L. Romyantsev, A. Arbuzov, R. Sadykov, and S. Bondarenko, *Phys. Rev. D* **98**, 013001 (2018).
- [44] S. Bondarenko, Ya. Dydyshka, L. Kalinovskaya, R. Sadykov, and V. Yermolchik [Phys. Rev. D (to be published)].
- [45] C. Carloni Calame, C. Lunardini, G. Montagna, O. Nicrosini, and F. Piccinini, *Nucl. Phys.* **B584**, 459 (2000).
- [46] C. M. Carloni Calame, *Phys. Lett. B* **520**, 16 (2001).
- [47] G. Balossini, C. M. Carloni Calame, G. Montagna, O. Nicrosini, and F. Piccinini, *Nucl. Phys.* **B758**, 227 (2006).
- [48] G. Balossini, C. Bignamini, C. Calame, G. Montagna, O. Nicrosini, and F. Piccinini, *Phys. Lett. B* **663**, 209 (2008).
- [49] S. Jadach, B. Ward, and Z. Was, *Phys. Rev. D* **88**, 114022 (2013).
- [50] A. Andonov, D. Bardin, S. Bondarenko, P. Christova, L. Kalinovskaya, and G. Nanava, *Fiz. Elem. Chastits At. Yadra* **34**, 1125 (2003) [*Phys. Part. Nucl.* **34**, 577 (2003)], <https://arxiv.org/pdf/hep-ph/0207156.pdf>.
- [51] G. Moortgat-Pick *et al.*, *Phys. Rep.* **460**, 131 (2008).
- [52] N. Davidson, G. Nanava, T. Przedzinski, E. Richter-Was, and Z. Was, *Comput. Phys. Commun.* **183**, 821 (2012).
- [53] A. Arbuzov, S. Bondarenko, and L. Kalinovskaya, *Symmetry* **12**, 1132 (2020).
- [54] S. G. Bondarenko and A. A. Saprosov, *Comput. Phys. Commun.* **184**, 2343 (2013).
- [55] A. Arbuzov, D. Bardin, S. Bondarenko, P. Christova, L. Kalinovskaya, U. Klein, V. Kolesnikov, L. Romyantsev, R. Sadykov, and A. Saprosov, *JETP Lett.* **103**, 131 (2016).
- [56] R. Sadykov and V. Yermolchik, *Comput. Phys. Commun.* **256**, 107445 (2020).
- [57] A. Belyaev, N. D. Christensen, and A. Pukhov, *Comput. Phys. Commun.* **184**, 1729 (2013).
- [58] M. Moretti, T. Ohl, and J. Reuter, [arXiv:hep-ph/0102195](https://arxiv.org/abs/hep-ph/0102195).
- [59] W. Kilian, T. Ohl, and J. Reuter, *Eur. Phys. J. C* **71**, 1742 (2011).
- [60] W. Kilian, F. Bach, T. Ohl, and J. Reuter, [arXiv:1403.7433](https://arxiv.org/abs/1403.7433).
- [61] J. Reuter, S. Brass, P. Bredt, W. Kilian, T. Ohl, V. Rothe, and P. Stenemeier, [arXiv:2002.06122](https://arxiv.org/abs/2002.06122).
- [62] J. Fleischer, J. Gluza, A. Lorca, and T. Riemann, *Eur. Phys. J. C* **48**, 35 (2006).
- [63] S. D. Badger, E. N. Glover, V. V. Khoze, and P. Svrcek, *J. High Energy Phys.* **07** (2005) 025.
- [64] D. Maître and P. Mastrolia, *Comput. Phys. Commun.* **179**, 501 (2008).
- [65] S. Bondarenko, Y. Dydyshka, L. Kalinovskaya, L. Romyantsev, R. Sadykov, and V. Yermolchik, *Phys. Rev. D* **100**, 073002 (2019).
- [66] C. Schwinn and S. Weinzierl, *J. High Energy Phys.* **04** (2007) 072.
- [67] E. P. Wigner, *Rev. Mod. Phys.* **29**, 255 (1957).
- [68] E. P. Wigner, *Phys. Today* **17**, 34 (1964).